NUMERICAL INVESTIGATION OF BI-COMPONENT DROPLETS VAPORIZATION IN A TURBULENT FLOW

Abou Al-Sood M.M.* and Ahmed M.
*Author for correspondence
Department of Mechanical Engineering,
Assiut University,
Assiut, 71516,
Egypt,
E-mail: m_aboualsood@hotmail.com

ABSTRACT

The purpose of this paper is to develop a three-dimensional (3D) numerical model capable of investigating the vaporization rate of bi-component liquid fuel droplets exposed to a convective turbulent gaseous air freestream at ambient room temperature and atmospheric pressure conditions. Droplets of n-heptane and n-decane mixtures with different compositions are used. The mathematical model is based on 3D Reynolds-Averaged Navier-Stokes equations, together with the mass, species, and energy conservation equations in gas phase whileas Navier-Stokes equations, mass, species, and energy conservation in the liquid phase. The turbulence terms in the conservation equations of the gas-phase are modelled by using the shear-stress transport (SST) model. A Cartesian grid based blocked-off technique is used in conjunction with the finite-volume method to solve numerically the governing equations of the gas and liquid-phases. The present predictions showed good agreement with turbulent experimental data available in the literature. The present study is limited to ambient room temperature and atmospheric pressure conditions.

INTRODUCTION

The evaporation of fuel droplets is fundamentally and practically important for many engineering systems. For example, the vaporization rate of liquid fuel is the controlling parameter in liquid-fuelled combustion systems in terms of efficiency and low pollutant emissions. Therefore, studying and understanding the vaporization of a liquid fuel droplet is a prerequisite for understanding the complex spray flows. Due to its importance, a number of studies and textbooks have been published, for example [1–3] among many others, while recent extended reviews are reported in[4–7].

Typical fuels consist of a mixture of two or more pure liquids with completely different physical and chemical properties [8, 9]. The degree of volatility, boiling temperature, evaporation latent heat, surface tension, and heat capacity of each component play an important role in the interior thermo-fluid dynamics of droplet. There are various complications that occur during vaporization of multicomponent liquid droplets. Different components vaporize at different rates, creating concentration gradients within droplets and causing mass diffusion. The evaporation characteristics of multicomponent droplets have been studied analytically, numerically, and experimentally [8-21]]. Most of existing studies on multicomponent droplets are subjected to stagnant or laminar forced convection. According to authors' knowledge, the only exception is the study of Birouk and Gökalp [17]. They investigated experimentally the vaporization rate of multicomponent droplets subjected to zero-mean velocity turbulence flows in terms of turbulent Reynolds number and Schmidt number.

The main objective of the present study is to develop a 3D model for investigating the effect of turbulence on vaporization of bi-component liquid fuel droplets (mixtures of *n*-heptane and *n*-decane) subjected to turbulence convective flows at ambient room temperature and atmospheric pressure. However, in most practical spray flow applications droplets evaporate under high-pressure and a hot turbulent environment. Therefore, an extension of this study to evaluate the effects of pressure and temperature will make it more practical.

NOMENCLATURE

A	[m^2]	cross section area
D	[m^2/s]	Diffusion conductance
d	[m]	Droplet diameter

h_{evap}	[J/kg.K]	latent heat of vaporization
I	[--]	turbulence intensity ($\sqrt{\overline{u'^2}}/U_\infty$)
k	[m²/s²]	turbulence kinetic energy
K	[mm²/s]	evaporation rate
L	[m]	length of the computational domain
$\dot{m}$	[kg/s]	mass flow rate
$\dot{m}''_{evap}$	[kg/s.m²]	rate of evaporated mass flux
Pe	[--]	Peclet number
p	[Pa]	pressure
S_ϕ	[--]	source term ($S_\phi = S_C + S_P\phi$)
t	[s]	time
U_∞	[m/s]	freestream velocity
U	[m/s]	velocity component in x-direction
V	[m/s]	velocity component in y-direction
W	[m/s]	velocity component in z-direction
Y_f	[--]	fuel mass fraction

Greek Letters

ϕ		diffusion parameter (U, V, W, p, k, and ω)
μ	[Pa.s]	molecular viscosity
μ_t	[Pa.s]	turbulence viscosity
ρ	[kg/m3]	density
α	[--]	convection weighting factor
β	[--]	diffusion weighting factor
Γ	[--]	generalized diffusion coefficient
λ	[W/m.K]	thermal conductivity
τ	[Pa]	shear stress
Δx	[m]	control volume length in x-direction
Δy	[m]	control volume length in y-direction
Δz	[m]	control volume length in z-direction

Subscripts

i	x-, y-or z-coordinates if (i=1, 2, or 3)
B	bottom (i,j,k-1) node
E	east (i+1, j, k) node
g	gas
l	liquid
N	north (i,j+1,k) node
P	center (i, j, k) node
S	south (i, j-1, k) node
T	top (i, j, k+1) node
W	west (i-1, j, k) node
b	control volume bottom (i,j,k-1/2) face
e	control volume east (i+1/2,j,k) face
eff	effective
n	control volume north (j+1/2) face
s	control volume south (i,j-1/2,k) face
t	control volume top (i,j,k+1/2) face
w	control volume west (i-1/2,j,k) face; wall

DESCRIPTION OF PHYSICAL MODEL

Consider a liquid droplet with an initial radius r_0 and initial temperature T_0 immersed into laminar or turbulent inert flow (air in the present study) of infinite expanse. The gas phase is prescribed by U_∞, p_∞, T_∞, $Y_{F\infty}$ and I_∞. The physical geometry of the problem with the initial and boundary conditions are illustrated in Figure 1.

The liquid droplet is stationary and immersed at a uniform temperature. Energy in the form of heat is transferred from the gas phase to the liquid phase. Initially, a fraction of this energy is used to heat-up the interior of the droplet, and the remainder is used for droplet's evaporation. Once the droplet surface temperature reaches its steady-state value, all the heat received by the droplet is then used for evaporation only. The evaporation of the liquid droplet (i.e. mass transfer) yields a decrease in the droplet radius. The evaporated mass is then diffused and convected away from the droplet surface and hence the gas phase becomes a mixture of fuel vapour and air.
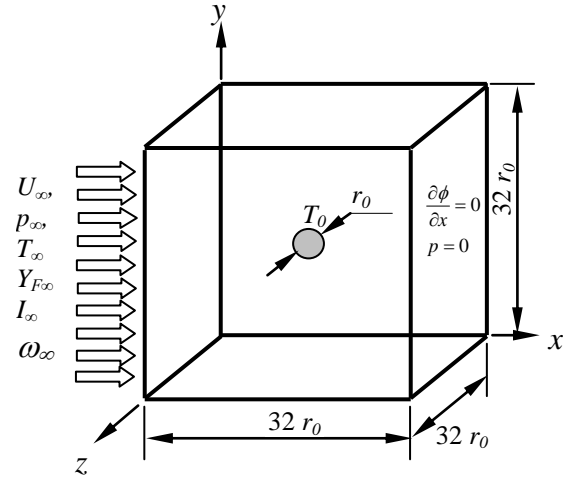

Figure 1 Physical problem with initial and boundary conditions of turbulent flow around a liquid droplet

Model Assumptions

The following assumptions are introduced in the present model: (i) The droplet contains only two components of hydrocarbon fuel (*n*-heptane and *n*-decane) with no chemical activity with the surrounding gas; (ii) Droplet's shape remains spherical, i.e. Weber number is much less than unity; (iii) Incompressible, steady and turbulent airflow with prescribed freestream turbulence intensity; (iv) Second order effects such as Dufour effect (energy flux due to mass concentration) and Soret effect (mass diffusion due to temperature) are considered negligible; and (v) Radiation and solubility of the ambient gas phase into liquid phase are also neglected.

Governing Equations

The governing equations for the gas-phase are the conservation of mass, momentum (i.e. Reynolds-Averaged Navier-Stokes), energy, species concentration, and turbulence kinetic energy and its dissipation rate. As for the liquid phase, the governing equations are those of mass, momentum and energy. The set of governing equations for the gas and the liquid phases can be conveniently written in a general transport equation form as follows:

$$\frac{\partial}{\partial t}(\rho\Phi) + \mathrm{div}(\rho u_i \Phi) = \mathrm{div}\{\Gamma_\Phi \mathrm{grad}\Phi\} + S_\Phi \qquad (1)$$

where the general variable Φ may represent the mean value of mass, any of the instantaneous velocity components (u, v, w), temperature T, mass fraction of the evaporating liquid fuel Y_F, turbulence kinetic energy k or dissipation per unit of kinetic energy ω. Γ_Φ represents an effective diffusion coefficient of

the general variable Φ, and S_Φ is the source term. This generalized transport equation contains four terms, i.e. transient, convection, diffusion and source term. The source term includes all terms that are not explicitly accounted for in the first three terms [22]. Closure for turbulence terms in the gas-phase governing equations is obtained by using the two-equation eddy-viscosity shear-stress transport (SST) model of Menter [23]. Validation of the numerical model revealed that the SST model produces the best predictions compared to all two-equation eddy-viscosity models [24, 25].

NUMERICAL METHOD

In order to solve the complex nonlinear and strongly coupled set of governing transport equations, a finite volume approach was employed [26]. The governing differential equations were integrated over discrete volumes resulting in a set of algebraic equations of the following general form

$$a_P \Phi_P = a_E \Phi_E + a_W \Phi_W + a_N \Phi_N + a_S \Phi_S + a_T \Phi_T + a_B \phi_B + b_\phi,$$
(2)

where a_P, a_E, a_W, a_N, a_S, a_T, a_B, and b_ϕ are coefficient which are defined as

$$a_p = a_E + a_W + a_N + a_S + a_T + a_B - S_P \Delta x \Delta y \Delta z$$
$$a_E = \beta_e D_e + \dot{m}_e \alpha_e - \dot{m}_e / 2$$
$$a_W = \beta_w D_w + \dot{m}_w \alpha_w + \dot{m}_w / 2$$
$$a_N = \beta_n D_n + \dot{m}_n \alpha_n - \dot{m}_n / 2$$
$$a_S = \beta_s D_s + \dot{m}_s \alpha_s + \dot{m}_s / 2$$
$$a_T = \beta_t D_t + \dot{m}_t \alpha_e - \dot{m}_t / 2$$
$$a_B = \beta_b D_b + \dot{m}_b \alpha_b + \dot{m}_b / 2$$
$$b_\phi = S_C \Delta x \Delta y \Delta z$$
(3)

where

$$\alpha_i = (1/2)(Pe)_i^2 / [5 + (Pe)_i^2],$$
$$D_i = 2\Gamma_i A_i / (\Delta x_I + \Delta x_P),$$
$$\Gamma_i = \Gamma_P \Gamma_I / [\Gamma_I \Gamma_P + (1 - f_i)\Gamma_I],$$
$$f_i = (\Delta x_j)_I / [(\Delta x_j)_I + (\Delta x_J)_P],$$
$$\beta_i = [1 + 0.005(Pe)_i^2 / [1 + 0.05(Pe)_i^2],$$
$$(Pe)_i = \dot{m}_i / D_i.$$

The subscripts P, E, W, N, S, T and B refer to center point of, east, west, north, south, top and bottom control volumes, while e, w, n, s, t and b refer to east, west, north, south, top and bottom face of the central control volume denoted as P. S_P and S_C are the coefficients of the linearized source term, i.e. $S_\Phi = S_C + S_P \Phi$ and f_i is the ratio of the neighbourhood node length to the total length of neighbourhood and central nodes in x, y or z direction with $f = 0.5$ if the grid is uniform. In the

equations above, $\Delta x_j = \Delta x$ for $j = 1$, Δy for $j = 2$ and Δz for $j = 3$. Finally, subscripts I and i above denote E, W, N, S, T or B and e, w, n, s, t or b, respectively.

In working numerically with the so-called primitive variables U, V, W and P, the absence of an explicit equation for pressure presents a difficulty. This difficulty was overcome by using the SIMPLEC approach of Van Doormall and Raithby [27] in which an expression in the form of Eq. (2) was derived for the pressure through a combination of the continuity and momentum equations. The ultimate goal is to develop a pressure field such that the resulting velocity field satisfies the continuity equation for every control volume in the calculation domain. The solution of the set of linearized algebraic equations described above was accomplished by using a three dimensional vectorized version of SIP (Strongly Implicit Procedure) developed by Leister and Perić [28]. The Strongly Implicit Procedure was chosen as a solver as it takes less number of iterations (less time) for convergence compared to other solvers such as SOR (successive over relaxation) or TDM (tri-diagonal matrix). The iterative procedure sweeps of the solution domain (gas phase or liquid phase) was continued until one of the two imposed conditions was achieved; either the assigned maximum number of iterations was exceeded or the range-normalized relative errors of the parameters (U, V, W, p, T, k, and ε) were satisfied for each control volume as $|\Phi^{n+1} - \Phi^n| / |\Phi_{max} - \Phi_{min}| \le \varepsilon_\Phi$ where Φ_{max} and Φ_{min} are the maximum and minimum values for the whole Φ^{n+1} field and ε_Φ was taken 10^{-4} for all quantities.

Freestream and Gas-Liquid Interface Conditions

The freestream mean velocity components, pressure, temperature, fuel mass fraction and turbulence quantities at the inlet of the computational domain are taken as $U = U_\infty, V = 0, W = 0$, $p = p_\infty$, $T = T_\infty$, $Y_F = 0$, $k = k_\infty$ and $\omega = \omega_\infty$. The freestream k_∞ and ω_∞ are estimated by using the following relations: $k_\infty = 1.5(I_\infty \times U_\infty)^2$ and $\omega_\infty = \rho_\infty (k_\infty / \mu_\infty)(\mu_{t\infty} / \mu_\infty)^{-1}$ [23, 29], where $\mu_{t\infty}$ is the freestream turbulent viscosity which is found approximately equal to μ_∞.

A distinctive gas-liquid interface exists at the droplet surface for which conditions were obtained by coupling the conservation equations (momentum, energy and species equations) in the gas and the liquid phases as
Shear stress continuity:

$$\mu_{eff} \left.\frac{\partial U_i}{\partial x_i}\right|_g = \mu \left.\frac{\partial U_i}{\partial x_i}\right|_l$$
(4)

Tangential velocity continuity:

$$U_i|_g = U_i|_l = U_s$$
(5)

Normal velocity continuity (non-slip condition):

$$U_j|_g = U_j|_l = 0$$
(6)

Temperature continuity:

$$T_g = T_l = T_s \qquad (7)$$

Energy conservation:

$$\lambda_t \left.\frac{\partial T}{\partial x_i}\right|_g = \lambda \left.\frac{\partial T}{\partial x_i}\right|_l + m''_{evap_i} h_{evap} \qquad (8)$$

Species conservation:

$$\dot{m}''_{evap_i}\left(Y_{f,g} - 1\right) - \rho_g D_{AB,g} \frac{\partial Y_{f,g}}{\partial x_i} = 0 \qquad (9)$$

Conservation of droplet mass:

$$\dot{r} = \frac{\sum_i \dot{m}''_{evap,i} A_i}{4\pi\rho\, r^2} - \frac{\pi\, r}{3\rho}\frac{d\rho}{dt} \qquad (10)$$

In the above equations, the subscripts g and l denote the gas phase and liquid phase at the droplet interface, respectively. The symbol $\dot{r}$ denotes the regression rate of the spherical droplet surface, r is the instantaneous droplet radius and A is the surface area of the nodes (represent the droplet surface) subjected to the flow. In the case of ambient atmospheric pressure and room temperature conditions, which is the case of the present study, the density variation term in Eq. (10) can be neglected as the change in density with time is insignificant.

Block-off Technique

The difficulty in developing a 3D numerical code lies in the creating a 3D computational grid especially in spherical coordinates. Many attempts have been made to overcome this difficulty and these include: first, transforming Navier-Stokes equations to general coordinates (ξ, η, and ζ) to be able to use the Cartesian grid [30-33]. This approach changes the original forms of Navier-Stokes (N-S) equations to more complicated forms that makes the discretization process more difficult by using finite-volume scheme. Second, using immersed-boundary fitted approach [34], which is based on introducing a body in the flow field of interest. This virtual body is a sort of momentum forcing in the Navier-Stokes rather than the real body, and therefore, flow over complex geometry can be easily handled with orthogonal grids (Cartesian or Cylindrical). The third technique is called blocking-off procedure, which consists of using a calculation domain that includes both the gas and liquid phase regions, and or blocking off the control volumes of an inactive region. The blocking-off procedure was first developed by Patankar [35] to compute flows in curvilinear geometries with a regular grid and to solve a conjugate heat transfer problem in a duct. Then, it was successfully extended to solve radiative heat transfer problems in irregular geometries using Cartesian coordinates. These radiative heat transfer studies dealt with two-dimensional problems [37-40], and three-dimensional problems [41-43]. Recently, this technique was used in medical studies [45] dealing with three-dimensional light and heat transport in several typical tissue domains with either one single blood vessel or two countercurrent blood vessels running through. These works show that the interest in this approach was for its result quality, ease of implementation, simplicity, and ease of grid generation compared to unstructured or multi-block grid generation.

Treatment of the Liquid Droplet in the Calculation Domain

This section describes the manner in which a spherical liquid fuel droplet is treated by the blocking-off method [46]. This method consists of blocking of the control volume within the spherical droplet of the calculation domain that includes both gas (air) and liquid droplet. The Cartesian-based blocked-off treatment of a droplet (spherical shape) immersed in the computational domain is schematically sketched in Figure 2. The treatment was accomplished by blocking-off the control volumes of the regular grid forming the droplet so that the remaining active control volumes form the desired computational domain in the gas phase. If the interest is the droplet, then the control volumes within the droplet are active and the others outside, i.e. in the gas phase, are inactive. It is obvious that the droplet was approximated by a series of parallel rectangulars or cubes. Figure 3 shows the regions *A* and *B* which represent the active and inactive control volumes, respectively. Although the computation was executed for the entire domain, only the solution within the active control volumes was meaningful. The blocking-off procedure consisted of giving values for the relevant functions in the inactive control volumes. A simple way in which the desired value could be obtained in the inactive control volumes was by assigning a large source term in the discretized equations. For example, setting S_C and S_P in the lierarized source term equation mentioned above for the internal grid points, i.e. the inactive zone, as $S_C = 10^{30}\phi_{P,desired}$ and $S_P = 10^{30}$, where 10^{30} denotes a number large enough to make the associated terms in the discretized equation negligible. Hence $S_C + S_p\Phi_P = 0$ so that $\Phi_P = -S_C / S_p = \Phi_{P,desired}$. Note that this procedure can be easily used to represent any irregular shaped object in the computation domain by inserting these internal boundaries conditions.
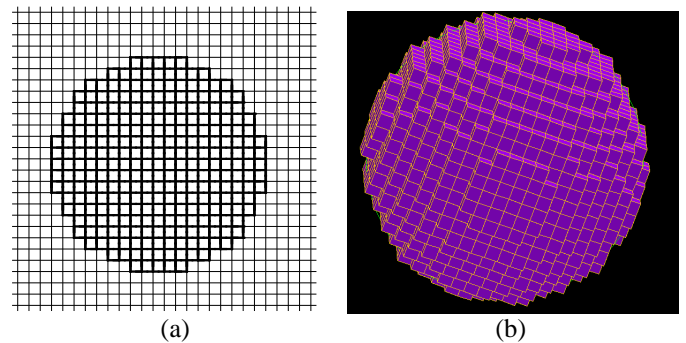

(a)   (b)

Figure 2 Cartesian-based blocked-off treatment of a droplet immersed in the computational domain (a) droplet in x-y plane, (b) droplet in 3D

Solution Procedure

The calculation domain was a cube of $32r \times 32r \times 32r$, where r is the droplet radius. The choice of the length of the cube is based on the suggestions made by Sundaarrajan and Ayyaswamy [47] who indicated that the freestream conditions must be at least ten times the droplet radius. This is because the location of the freestream conditions may affect the numerical solution as the pressure correction equation is elliptical in nature. The computation domain was divided into control volumes and the droplet was generated at the centre. Figure 1 summarizes the computational domain and the boundary conditions as, the left and right faces are inflow and outflow boundary conditions, respectively. The other faces, north, south, top, and bottom, were taken as the wall boundary conditions. In the present analysis, the Cartesian grid in the calculation domain consisted of 60x60x60. Since the gradients around the droplets were large, a very fine grid 40x40x40 was used in the domain $2r$ from the sphere centre in all directions, as shown schematically in Figure 4.
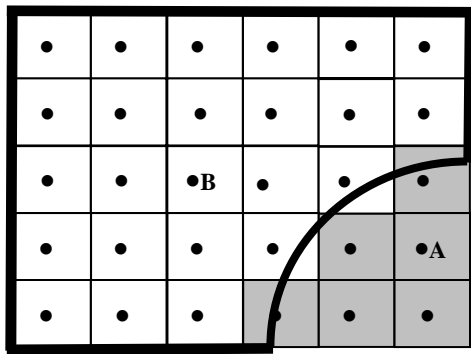
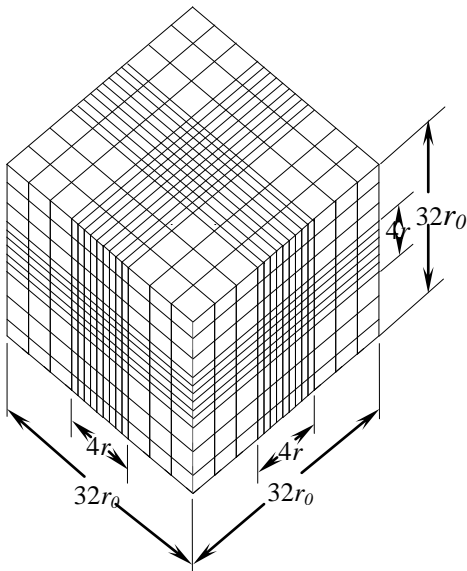**Figure 3** Schematic of Blocked-off regions (active and inactive) in Cartesian grid

Figure 4 Schematic diagram of the computational grid

RESULTS AND DISCUSSIONS

Validation of the Numerical Model

The current three-dimensional numerical model is validated first by comparing the present numerical predictions with the existing published experimental and numerical laminar data. The present laminar predictions are obtained by assigning a value of zero to the freestream turbulence intensity in the numerical code. Figures 5, 6 display a typical variation of the time-history of the squared normalized diameter of n-heptane and n-decane droplets, respectively, in freestream of air having a mean-velocity of $U_\infty = 2.5$ m/s. These figures show that the present predictions agree reasonably well with published numerical data [48] and almost perfectly with experimental data [49]. Laminar evaporation of a droplet consisting of 50% n-heptane-50% n-decane mixture is shown in Figure 7. Also, this figure shows the good comparisons of the present model with published numerical and experimental data available in the open literature.
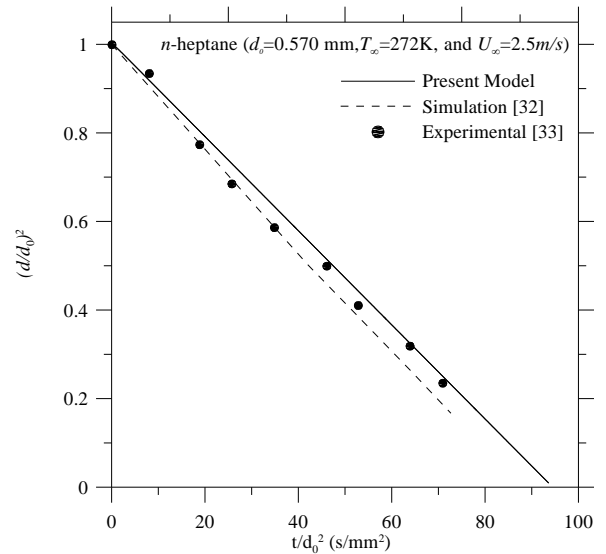

Figure 5 Time-history of the squared normalized diameter for n-heptane droplet in a laminar flow
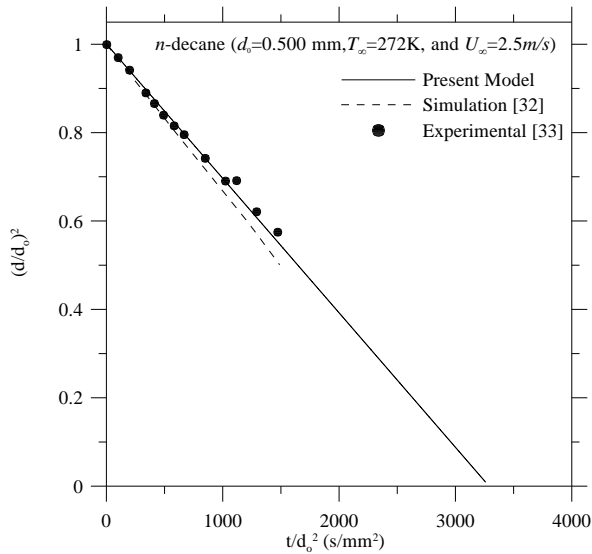
Figure 6 Time-history of the squared normalized diameter for *n*-decane droplet in a laminar flow

Unfortunately, there is no data available in the literature for the evaporation of bi-component droplets under turbulent flow conditions. So, the present model is compared (in case of turbulent flow) only for single component droplets. Figure 8 illustrates the predicted vaporization rate of *n*-heptane and *n*-decane droplets under turbulent flow conditions and its comparison with published experimental data [34]. This figure shows that the present numerical predictions obtained with the SST closure model agree reasonably well with their counterparts' experimental data within acceptable experimental error.
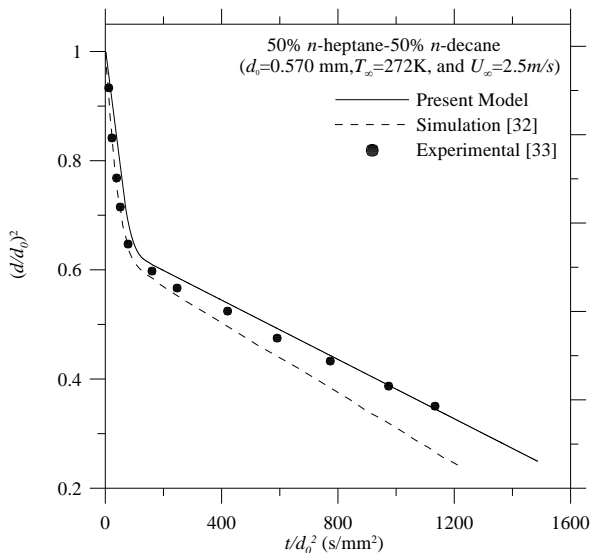

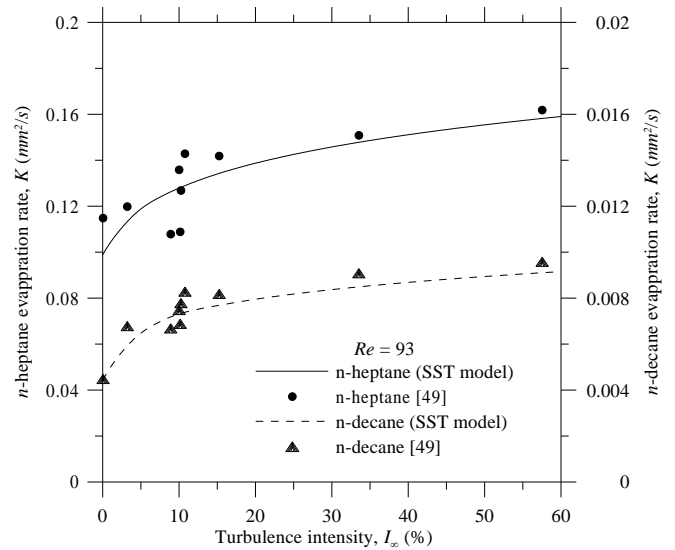**Figure 7** Time-history of the squared normalized diameter for *n*-heptane-*n*-decane droplet in a laminar flow

Figure 8 Time-history of *n*-heptane and *n*-decane droplets evaporation rates for different airstream turbulence intensities

Evaporation of a Pure Liquid Droplets in Forced Laminar and Turbulent Flows

The test conditions employed in the present study are limited to those reported in Table 1.Two examples are given in Figures 9, 10 which show the time-history of the squared normalized diameter of *n*-heptane and *n*-decane droplets, respectively, versus the normalized evaporation time for laminar airstream, as well as for various airstream turbulence intensities. The droplet life time is terminated when 99.9% of the droplet is evaporated. After the elapse of the droplet heating-up period, the squared droplet diameter appears to follow a linear variation with the evaporation time obeying the famous d^2-law. Moreover, this figure clearly shows that turbulence decreases the life time of the droplet yielding an increase in the droplet mass transfer (i.e. the evaporation rate).
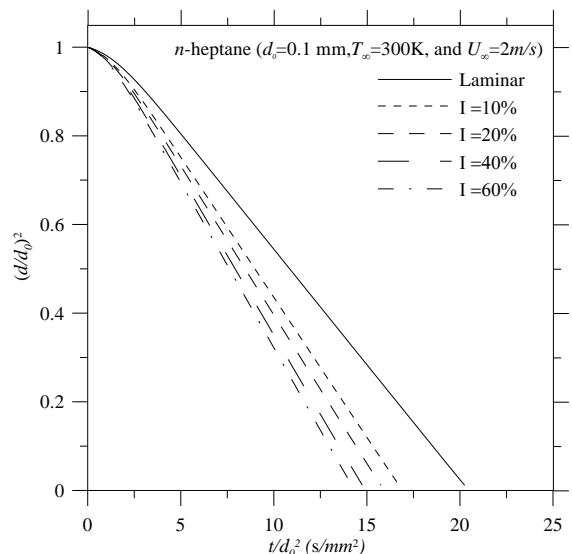

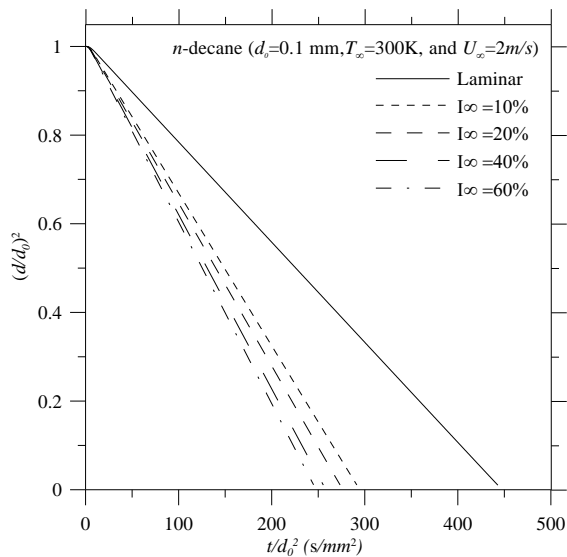**Figure 9** Time-history of the squared normalized diameter of *n*-heptane droplet

Figure 10 Time-history of the squared normalized diameter of *n*-decane droplet

Evaporation of Bi-Component Droplets in Forced Laminar and Turbulent flows

Turbulent vaporization of bi-component droplets of mixture of n-heptane and *n*-decane is investigated by the present model for the same test conditions listed in Table 1. The investigated mixtures contain, respectively, 30, 50, and 70% n-decane by volume. Typical variations of the time-history of the squared normalized diameter of a droplet with the initial composition mentioned above are shown in Figures 11, 12, 13, respectively. These figures reveal that the droplet evaporation took place in two phases for all turbulence intensities. The first phase corresponds to the evaporation of most of heptane (low volatile), and the second phase corresponds to the evaporation of the remaining droplet. Also, it is noted that most of turbulence effect happens at moderate turbulence intensity ($\approx 20\%$).
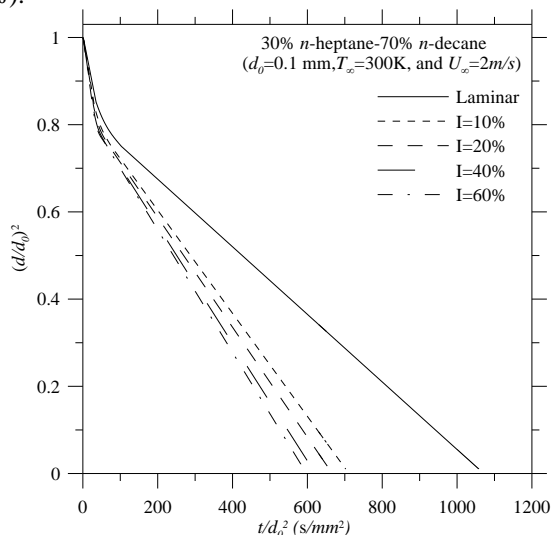

Figure 11 Time-history of $(d/d_0)^2$ of 30% *n*-heptane-70% *n*-decane droplet subjected to turbulent flows
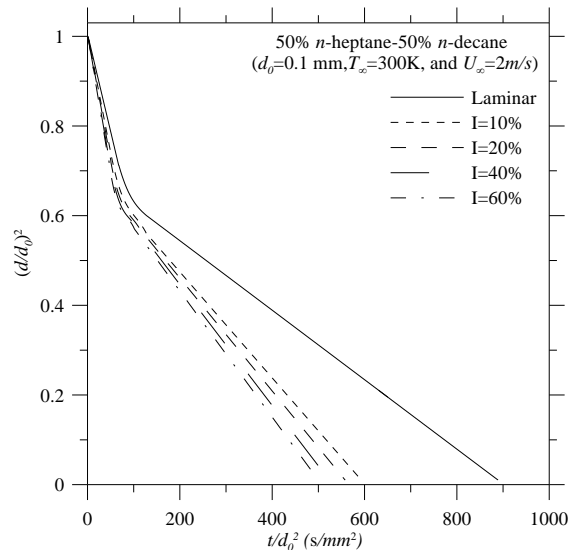

Figure 12 Time-history of $(d/d_0)^2$ of 50% *n*-heptane-50% *n*-decane droplet subjected to turbulent flows
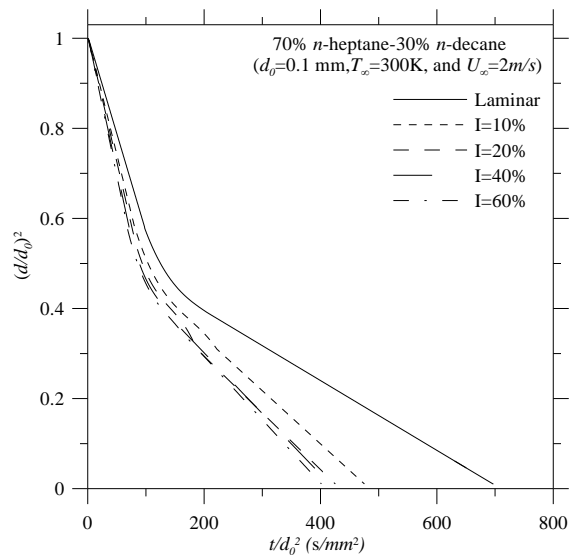

Figure 13 Time-history of $(d/d_0)^2$ of 70% *n*-heptane-30% *n*-decane droplet subjected to turbulent flows

When comparing the pure *n*-heptane droplet vaporization results with first phase of vaporization for the bi-component droplet under the same flow conditions, the vaporization rate for bi-component droplet is significantly less that the pure *n*-heptane droplet. This observation indicates that the surface layer of the bi-component droplet is not made up of pure *n*-heptane. The vaporization rates of the second stage of vaporization for bi-component droplets are identical to that of pure *n*-decane droplets under the same flow conditions.

CONCLUSION

A 3D model is developed to investigate the rate of mass transfer from bi-component liquid fuel droplets in forced convective turbulent flow at atmospheric pressure and room temperature conditions. This model is based on Reynolds-Averaged Navier-Stokes equations, together with the mass, species, and energy conservation equations in conjunction with turbulence closure model (SST model) in gas phase whileas Navier-Stokes equations, mass, species, energy conservation, in the liquid phase. Bi-component droplet vaporization took place in two stages for all turbulence intensities. The first stage corresponds to the evaporation of most of heptane (low volatile), and the second stage corresponds to the evaporation of the remaining droplet. When comparing the pure n-heptane droplet vaporization results with first stage of vaporization for the bi-component droplet under the same flow conditions, the vaporization rate for bi-component droplet is significantly less that the pure *n*-heptane droplet. This observation indicats that the surface layer of the bi-component droplet is not made up of pure *n*-heptane. The vaporization rates of the second stage of vaporization for bi-component droplets are identical to that of pure *n*-decane droplets under the same flow conditions.

REFERENCES

[1]   Clift, R, Grace, J.R., and Weber M.E., Bubbles, drops and particles,New York, Academic Press,1978

[2]   Sirignano, W.A., Fluid dynamics and transport of droplets and sprays. Cambridge, University Press, 1999

[3]   Bird, R.B, Stewart, W.E., and Lightfoot E.N., Transport phenomena. 2$\underline{^{nd}}$ ed. New,York, Wiley, 2002

[4]   Givler, S.D., and Abraham, J., Supercritical droplet vaporization and combustion studies, *Prog Energy Combust Sci* , vol. 22, 1996, pp 1–28

[5]   Miller, R.S., Harstad, K., Bellan, J., Evaluation of equilibrium and non-equilibrium evaporation models for many-droplet gas–liquid flow simulations, *Int J Multiphase Flow*, Vol 24, 1998, pp.1025–1055

[6]   Bellan J., Supercritical (and subcritical) fluid behavior and modeling: drops, streams, shear and mixing layers, jets and sprays. *Prog Energy Combust Sci* , Vol. 26, 2000, pp. 329–466.

[7]   Sazhin ,S.S., Advanced models of fuel droplet heating and evaporation, *Prog Energy Combust Sci*, Vol. 32, 2006, pp.162–214

[8]   Law C.K, Multicomponent droplet combustion with rapid internal mixing, Combust Flame, Vol. 26, 1976, pp. 26:219–333

[9]   Law K., Prakash S., Sirignano W.A. , Theory of convective, Transient, multicomponent droplet vaporization, *Proceedings of the 16th Symposium on Internal Combustion,* 1977, pp. 605-617

[10]   Sirignano A., and Law C.K., Transient heating and liquid phase mass diffusion in droplet vaporization, *Adv. Chemistry Series*, vol. 166, 1978, pp. 1-2

[11]   Law, C.K., Internal boiling and superheating in vaporizing multicomponent droplets, *AIChE J* , Vol. 24, 1978, pp.626–632

[12]   Maqua, C., Castanet, G., and Lemoine, F., Bicomponent droplets evaporation: temperature measurements and modeling, *Fuel*, Vol. 87, 2008, pp. 2932–2942

[13]   Tong, A.Y., Sirignano, W.A., Multicomponent transient droplet vaporization with internal circulation: integral equation formulation, Numer. Heat Transfer, Vol. 10, 1986, pp. 253–278

[14]   Megaridis C.M, Sirignano, W.A., Multicomponent droplet vaporization in a laminar convective environment, *Combust Sci Technol*, Vol. 87, 1993, pp. 27–44

[15]   Daif, A., Bouaziz, M., Chesneau, X., and Ali Cherif, A., Comparison of multicomponent fuel droplet vaporization experiments in forced convection with the Sirignano model, *Exp. Thermal and Fluid Science*, Vol. 18, 1999, pp. 282-290

[16]   Aggrawal, S.K., and Mongia, H. C., Multicomponent and high-pressure effects on droplet vaporization, *J. Engineering for Gas Tur. And Power*, Vol. 124, 2002, pp. 248-255

[17]   Birouk, M., and Gökalp, I., A new correlation for turbulent mass transfer from liquid drops, Int. J. Heat Mass Transfer, Vol. 45, 2002, pp. 37-45

[18]   Arias-Zugasti, M., and Rosner, D.E., Multicomponent fuel droplet vaporization and combustion using spectral theory for a continuous mixture, *Combust. Flame*, Vol. 135, ,2003, 271-284

[19]   Sazhin, S.S., Elwardany, A., Krutitskii, P.A., Castanet, G., Lemoine, F., Sazhina, E.M., and Heikal, M.R., A simplified model for bi-component droplet heating and evaporation. Int J Heat Mass Transer, Vol. 53, 2010, pp.4495–4505

[20]   Ebrahimian, V., and Habchi, C., Towards a predictive evaporation model for multi-component hydrocarbon droplets at all pressure conditions, Int. J. Heat Mass Transfer, Vol. 54, 2011, pp. 3552-3565

[21]   Strotos G, Gavaises M, Theodorakakos A, and Bergeles G., Numerical investigation of the evaporation of two-component droplets, *Fuel,* Vol. 90, 2011, pp. 1492-1507

[22]   Abou Al-Sood, M. M., and Birouk, M., A numerical model for calculating the vaporization rate of of of a fuel droplet exposed to a convective turbulent flow, *Int. J. Numer. Methods Heat Fluid Flow*, Vol. 18, 2008, pp. 146-159

[23]   Menter, F.R. ,Two-equation eddy-viscosity turbulence models for engineering applications, *AIAA Journal*, Vol. 32,1994, pp. 1598-1605

[24]   Abou Al-Sood, M.M., *Simulation and Modelling of Liquid droplet's vaporization in turbulent flow*, PhD thesis, 2006, Manitoba University, Manitoba, Canada

[25]   Birouk, M., Abou Al-Sood, M.M., Numerical study of sphere drag coefficient in turbulent flow at low Reynolds number, *Num. Heat Transfer A*, Vol 51,2007, pp. 39-57

[26]   Patankar, S.V., *Numerical heat transfer and fluid flow, Hemisphere*, 1980

[27]   Van Doormall, J.P., and Raithby, G.D., Enhancement of the simple method for predicting incompressible fluid flows, *Numer. Heat Transfer*, Vol. 7 ,1984, pp. 147–163

[28]   Leister, H.-J., Peri´c, M., Vectorized strongly implicit solving procedure for a seven-diagonal coefficient matrix, *Int. J. Numer. Methods Heat Fluid Flow*, Vol. 4, 1994, pp. 159–172

[29]   Karel, L.D., Recent experience with deferent turbulence models applied to the calculation of flow over aircraft components, *Prog. Aerospace Sci.*, Vol. 34, 1998, pp. 481–541

[30]   Drikakis, D., Development and implementation of parallel high-resolution schemes in 3D flows over bluff bodies, *Proceedings of the Parallel CFD Conference Implementation and Results Using Parallel Computers*, Elsevier Science Publishers, Amsterdam, . 1995, pp 191–198

[31]   Johnson, T. A., Numerical and experimental investigation of flow past a sphere up to a Reynolds number of 300", Ph.D. dissertation, *University of Iowa*, USA, 1996

[32] Constantinescu, S.G., and Squires, K.D, Numerical investigation of the flow over a sphere in the subcritical and supercritical regimes, *Physics of Fluids*, Vol. 15, no. 5, 2004, pp. 1449-1467

[33] Niazmand, H., and Renksizbulut, M., Flow past a spinning sphere with surface blowing and heat transfer, *Journal of Fluids Engineering, Transactions of the ASME*, Vol. 127, no. 1, 2005, pp. 163-171

[34] Kim, J., Kim, D., and Choi, H., An immersed boundary Finite-Volume method for simulation of flow in complex geometries, *J. Comput. Phy.*, Vol. 171, 2001, pp. 35-60

[35] Patankar, S. V., A Numerical method for conduction in composite materials, flow in irregular geometries and conjugate heat transfer, *in Proc. 6th Int. Heat Transfer Conf.*, Toronto, Canada, Vol. 3, 1978, pp. 297-302.

[36] Patankar, S. V., Computation of conduction and duct flow heat transfer," *Innovative Research*, Inc., Minneapolis, MN. 1991

[37] Chai, J. C., Lee, H. S. and Patankar, S. V., Treatment of Irregular Geometries Using a Cartesian-Coordinates-Based Discrete-Ordinates-Method, Radiative Heat Transfer: Theory and Applications, HTD- Vol. 244, 1993, *ASME*, New York

[38] Kim, M. Y., Wook, S. W. and Park, J. H., Unstructured finite-volume method for radiative heat transfer in a complex two-dimensional geometry with obstacles, *Numerical Heat Transfer B*, Vol. 39, 2001, pp. 617-635

[39] Byung, D. Y., Baek, S. W., and Kim, M. Y., Investigation of radiative heat transfer in complex geometries using blocked-off , multiblock, and embedded boundary treatments, *American Society of Mechanical Engineers, Heat Transfer Division*, Vol. 366, 2000, pp. 119-126

[40] Byung, D. Y., Baek, S. W. and Kim, M. Y., Prediction of radiative Heat Transfer in a 2D enclosure with blocked-off, multiblock, and embedded boundary treatments, *Numerical Heat Transfer A*, Vol. 43, no. 8, 2003, pp. 807-825

[41] Coelho, P. J., Goncalves, J. M., Carvalho, M. G. and Trinic, D. N., Modelling radiative heat transfer in enclosures with obstacles," *Int. J. Heat Mass Transfer*, Vol. 41, 1998, pp. 745-756

[42] Borjini, M. N., Farahat., H., and Radhouani, M. S., Analysis of radiative Heat transfer in a partitioned idealized furnace," *Numerical Heat Transfer A*, Vol. 44, no. 2, 2003, pp. 199-218

[43] Consalvi, J. L., Porterie, B., and Lraud, J. C., Method for computing the interaction of fire environment and internal solid boundaries," *Numerical Heat Transfer A*, Vol. 43, no. 8, 2003, pp. 777-805

[44] Zhou, J. and Liu, J., Numerical study on 3-d light and heat transport in biological tissues embedded with large blood vessels during laser-induced thermotherapy", *Numerical Heat Transfer A*, Vol. 45, 2004, pp. 415-449

[45] Patankar, S. V., A Numerical method for conduction in composite Materials, flow in irregular geometries and conjugate heat transfer, *in Proc. 6th Int. Heat Transfer Conf.*, Toronto, Canada, Vol. 3, 1987, pp. 297-302

[46] Sundararajan, T. and Ayyaswamy, P. S., Hydrodynamics and heat transfer associated with condensation on a moving drop: solution of intermediate Reynolds number, *J. Fluid Mech.*, Vol. 149, 1984, pp. 33-58

[47] Longest, P.W, and Kleinstreuer, C, Computational models for simulating multicomponent aerosol evaporation in upper respiratory airways, j. Aerosol Sci., Vol. 39, 2005, pp. 124-138

[48] Runge, T., Meske, M., and Polymeropoulou, C. E., Low-temperature vaporization of JP-4 and JP-8 fuel droplets, *Atomization Sprays*, Vol. 8,1998, pp.25–44

[49] Wu, J–S., Lin Y–J. and Sheen, H–J., Effects of Ambient Turbulence and Fuel Properties on the Evaporation Rate of single Droplets, *Int. J. Heat Mass Transfer*, Vol. 44, 2001, pp. 4593-4603